Materials Chemistry and Physics 113 (2009) 515–517

Contents lists available at ScienceDirect

Materials Chemistry and Physics

journal homepage: www.elsevier.com/locate/matchemphys

Materials science communication

Characterization of 2024-T3: An aerospace aluminum alloy

Zainul Huda[a,*], Nur Iskandar Taib[b,1], Tuan Zaharinie[a,2]

[a] Department of Mechanical Engineering, University of Malaya, Kuala Lumpur, Malaysia
[b] Department of Geology, University of Malaya, Kuala Lumpur, Malaysia

ARTICLE INFO

Article history:
Received 29 January 2008
Received in revised form 4 July 2008
Accepted 21 September 2008

Keywords:
2024-T3 aluminum alloy
Microstructure
SEM
EPMA

ABSTRACT

The 2024-T3 aerospace aluminum alloy, reported in this investigation, was acquired from a local aerospace industry: Royal Malaysian Air Force (RMAF). The heat treatable 2024-T3 aluminum alloy has been characterized by use of modern metallographic and material characterization techniques (e.g. EPMA, SEM). The microstructural characterization of the metallographic specimen involved use of an optical microscope linked with a computerized imaging system using MSQ software. The use of EPMA and electron microprobe elemental maps enabled us to detect three types of inclusions: Al–Cu, Al–Cu–Fe–Mn, and Al–Cu–Fe–Si–Mn enriched regions. In particular, the presence of Al_2CuMg (S-phase) and the $CuAl_2$ (θ') phases indicated precipitation strengthening in the aluminum alloy.

1. Introduction

Advanced aluminum alloys for aerospace application are required to possess high fracture toughness, high fatigue performance, high formability, and superplasticity to meet the needs for lower structural weight, higher damage tolerance, and higher durability [1]. The heat-treatable 2024-T3 aluminum alloy, reported in this investigation, has attractive features of high strength and that its ductility does not significantly decrease during the strengthening heat treatment [2–4].

Microstructural characterization of metals and alloys usually employs optical and electron microscopy. Recent advances in scanning electron microscopy (SEM) enable us to conduct not only microstructural characterization but also precise elemental analysis with the aid of an electron probe micro-analyzer (EPMA) linked to the SEM [5–7]. An electron probe micro-analyzer (EPMA) is a microbeam instrument used primarily for the *in situ* non-destructive chemical analysis of minute solid samples. It is an analytical technique that is used to establish the composition of small areas on specimens. EPMA is one of several particle-beam techniques. Particular, although not unique, to EPMA is bombardment of the specimen with a beam of accelerated electrons. The electron beam is focused on the surface of a specimen using a series of electromagnetic lenses, and these energetic electrons produce characteristic X-rays within a small volume (typically between 1 and 9 μm^3) of the specimen [8].

The research reported in present paper presents microstructural and material characterization of *ALCLAD* sheet conforming to 2024-T3 aluminum alloy through metallographic investigations, optical microscopy, SEM, and EPMA techniques. *ALCLAD* is the aluminum alloy sheet coated with pure aluminum with coating thickness up to 0.01 mm; it is produced by sandwiching the base metal (2024-T3 aluminum alloy) between pieces of the coating metal (pure aluminum) and the sandwich is then rolled to the required thickness [9]. The *ALCLAD* 2024-T3 aerospace aluminum alloy (sheet) is extensively used in the skin of the C-130 Hercules aircrafts [10].

2. Experimentation

The starting material (SM) was in the form of *ALCLAD* sheet conforming to the 2024-T3 aluminum alloy; and was acquired from a local aerospace industry: Royal Malaysian Air Force (RMAF). Metallographic specimen for the SM was prepared by sectioning a small sample with scissors followed by coldmounting. The sample was ground by using emery papers on a metallographic grinding machine. Polishing was done with high-alumina powder on a metallographic polishing machine. The metallographic sample was etched with Kroll's reagent. The microstructural characterization involved use of both optical and scanning electron microscopes (SEM) as well as elemental distribution images and WDS-based quantitative spot analyses from an electron probe micro analyzer (EPMA) (*Cameca SX-100*). The photomicrographs were taken by use of an optical microscope linked with a computerized imaging system using MSQ software.

3. Results and discussion

The microstructures of the as-received material are shown as scanning electron micrograph (SEM) and optical micrograph in Fig. 1(a, b), respectively. Fig. 1(a) presents the SEM micrograph for

* Corresponding author. Tel.: +603 79674593; fax: +603 79675317.
E-mail addresses: drzainulhuda@hotmail.com (Z. Huda), ntaib@alumni.indiana.edu (N.I. Taib), rinie_3483@hotmail.com (T. Zaharinie).
[1] Tel.: +60 37967 4154.
[2] Tel.: +60 1261293176.

0254-0584/$ – see front matter © 2008 Elsevier B.V. All rights reserved.
doi:10.1016/j.matchemphys.2008.09.050

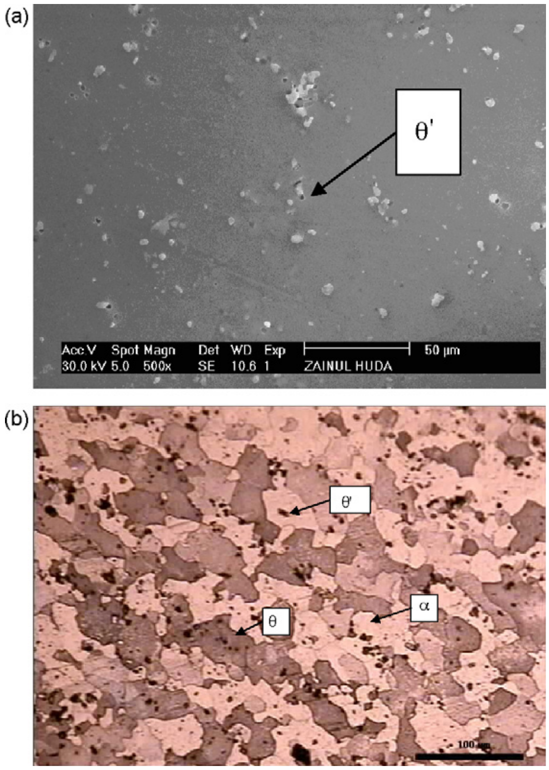

Fig. 1. (a): Scanning electron microscope of as-received material showing θ′ precipitates; and (b): Optical micrograph of as-received material: 2024-T3 aluminum alloy.

the aluminum alloy; which clearly shows precipitation of second-phase of θ′ phase in the aluminum matrix. The optical micrograph showing the multi-phase microstructure of the 2024-T3 aluminum alloy is shown in Fig. 1(b); this micrograph not only shows the α and θ phases but also the θ′ precipitates dispersed throughout the microstructure of the material. The α phase in the microstructure refers to the solid solution of copper and other alloying elements in the FCC (face centered cubic) lattice of aluminum; whereas the θ phase refers to the intermetallic compound conforming to the chemical formula: $CuAl_2$ [9,11–13]. Although both the θ phase and θ′ precipitates conform to the $CuAl_2$ formula, the distinction between the two phases is that the former appears as colonies of precipitates in the microstructure whereas the latter appears as dispersion of fine precipitates distributed throughout the microstructure (see Fig. 1(a, b)). The presence of θ′ precipitates also confirms that the material had been precipitation strengthened by the T-3 heat treatment for the aluminum alloy. The T-3 (temper-3) refers to a three-stage treatment: (1) solution treated, (2) cold-worked, and (3) tempered; given to the 2024 aluminum alloy [9].

The optical micrograph in Fig. 1(b) also allows computing of grain size of the as-received material; which was measured to be around 19.6 μm. A comparison of the grain size value for the investigated alloy with other engineering metals (e.g. [14,15]) indicate that the computed value of grain size (19.6 μm) for the 2024-T3 aluminum alloy is reasonably low i.e. the material is fine-grained. According to the Hall–Petch relationship, the tensile yield strength of a material varies inversely as its grain size [11,14]. Hence, it is quite logical to assume that the investigated 2024-T3 aluminum alloy possess good tensile strength.

The use of electron microprobe micro-analyzer (EPMA) facilitated with the *Cameca SX-100* microprobe enabled us to obtain

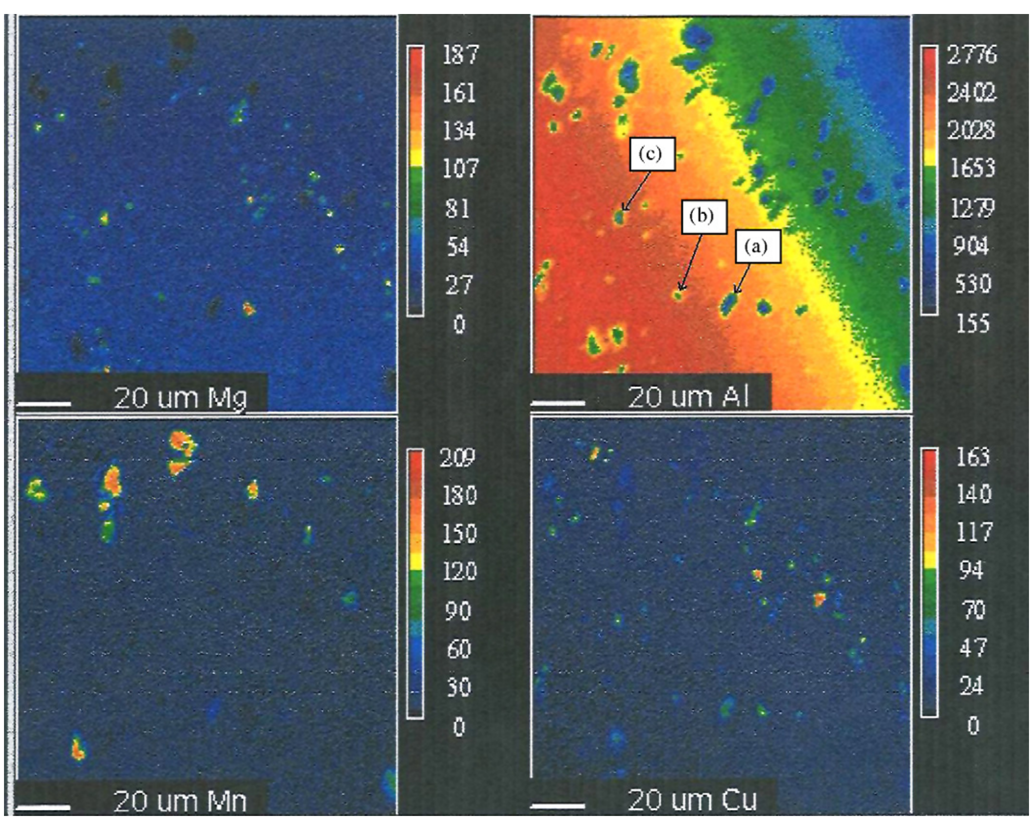

Fig. 2. Electron microprobe elemental mops for Al, Cu, Mg, and Mn. The colours correspond to count rates. The higher count rates indicate higher concentrations of the element (s) indicated. The spots marked as (a), (b), and (c) indicate regions containing Al, Cu; AJ, Mg; and Al, Cu, Mg, respectively.

Table 1
Chemical compositions (in wt.% and at.%) of second-phase particles in 2024-T3 aluminum alloy.

Element	Background metal		Al–Cu inclusions		Al–Cu–Fe–Mn inclusions		Al–Cu–Fe–Si–Mn inclusions	
	(1) wt.%	(2) at.%	(3) wt.%	(4) at.%	(5) wt.%	(6) at.%	(7) wt.%	(8) at.%
Al	91.4	94.5	58.7	76.1	54.2	70.8	47.4	61.6
Cu	5.5	2.4	39.7	21.9	22.5	12.5	20.7	11.4
Mg	2.4	2.7	1.2	1.7	–	–	–	–
Fe	–	–	–	–	14.5	9.1	14.5	9.1
Mn	–	–	–	–	5.5	3.5	5.9	3.7
Si	–	–	–	–	2.7	3.4	10.9	13.5
Total	99.3	99.6	99.6	99.7	99.4	99.3	99.4	99.3

the electron microprobe elemental maps for Al, Cu, Mg, and Mn (see Fig. 2); which shows regions containing high concentrations of various elements. For instance, the region marked '(a)' indicates high concentrations of Cu and Al; the mark '(b)' indicates region enriched in Mg and Al; and the mark '(c)' indicates region enriched in Al, Mg, and Cu. These regions/phases were spot analyzed using a 1-μm diameter beam, yielding the results presented in Table 1. The columns (1) and (2) in Table 1 represent the analyses of the background metal (aluminum alloy), which contains appreciable quantities of Cu and Mg. The columns (3) and (4) in Table 1 represent analyses of inclusions high in Al and Cu; these inclusions are marked as '(a)' in Fig. 2. The data in Table 1 enable us to identify three types of inclusions: (1) Al–Cu containing particles, (2) Al–Cu–Fe–Mn containing, and (3) Al–Cu–Fe–Si–Mn containing particles. A reference to the spots in Fig. 2 and the data in Table 1 lead us to conclude that the alloy is not entirely homogeneous, i.e. the alloy is chemically heterogeneous.

In view of the discussion in the preceding paragraph and a reference to literature [16–20], it is concluded that the alloy contains two major second-phase particles: (1) Al–Cu containing particle, i.e. $CuAl_2$ (θ′ phase), and (2) Al–Cu–Mg containing particle or Al_2CuMg, S phase. These second-phase particles serve to strengthen the alloy through a precipitation-strengthening mechanism, which involves obstructing movement of dislocations due the presence of the second-phase particles in the alloy [12,14,15]. Recently, Khan et al. have investigated precipitation strengthening in Al–Cu–Mg alloys; and have reported strengthening by the non-shearable S-phase precipitate in 2024-T351 aluminum alloy [21]. Hence, it is concluded that the investigated 2024-T3 aluminum alloy is strengthened by multiple-phase strengthening mechanisms (particularly, the θ′-phase and S-phase strengthening mechanisms); and hence possesses excellent strength.

4. Conclusions

The optical and scanning electron microscopy (SEM) for the investigated aluminum alloy enables us to confirm that the alloy had been heat treated according to the 2024-T3 three-stage treatment (solution treatment, cold-working, and tempering). The measured grain size (19.6 μm) and the interpretation of microstructures for the alloy led us to conclude that the alloy possesses good tensile strength. The analysis of elemental map from EPMA for the 2024-T3 aluminum alloy (ALCLAD sheet) confirmed the presence of three types of inclusions: Al–Cu, Al–Cu–Fe–Mn, and Al–Cu–Fe–Si–Mn enriched regions. The investigated alloy was found to be chemically heterogeneous. In particular, the presence of Al_2CuMg (S-phase) and $CuAl_2$ (θ′) phases in the alloy indicated multiple-phase strengthening in the 2024-T3 aluminum alloy. The electron probe micro-analysis and structure–property relationships enable us to conclude that the investigated 2024-T3 aluminum alloy possesses excellent tensile strength and is suitable for aerospace applications, particularly in the skin of aircrafts.

Acknowledgements

The authors are grateful to the Royal Malaysian Air Force (RMAF) for providing the research material: 2024-T3 aluminum alloy (ALCLAD sheet). The authors are also thankful to the Department of Geology, University of Malaya for permitting use of Electron Probe Micro Analyzer (EPMA).

References

[1] M. Nakai, T. Eto, Mater. Sci. Eng. A 285 (2000) 62.
[2] P. De Garmo, J.T. Black, R.A. Kohser, Materials and Processes in Manufacturing, John Wiley Publications, New York, USA, 2003.
[3] H. Kacer, E. Atik, C. Miric, J. Mater. Process. Technol. 142 (3) (2003) 762.
[4] J. Mao, S.B. Kang, J.O. Park, J. Mater. Process. Technol. 159 (3) (2005) 314.
[5] S.J.B. Reed, Electron Microprobe Analysis and Scanning Electron Microscopy in Geology, 2nd ed., Cambridge University Press, UK, 2005.
[6] J.I. Goldstein, D.E. Newbury, P. Echlin, D.C. Joy, C.E. Lyman, E. Lifshin, L.C. Sawyer, J.R. Michael, Scanning Electron Microscopy and X-Ray Microanalysis: A text for biologists, materials scientists, and geologists, 3rd ed., Plenum Press, N.Y., USA, 2003.
[7] M.H. Loretto, Electron Beam Analysis of Materials, Chapman and Hall Publishers, UK, 1993.
[8] S.J.B. Reed, Electron Microprobe Analysis, 2nd ed., Cambridge University Press, UK, 1993.
[9] R.A. Higgins, Engineering Metallurgy, 5th ed., Edward Arnold Publisher, UK, 1983.
[10] Personal communication with Engineers, Aircraft Repair Div, TUDM (Royal Malaysian Air Force), Subang, Malaysia, (2006).
[11] D.R. Askeland, P.P. Phule, The Science and Engineering of Materials, Thomson Books Inc., USA, 2003.
[12] I.J. Polmear, Light Alloys: Metallurgy of the Light Metals, Routledge Metallurgy and Materials Science Series, New York, USA, 1995.
[13] E. Marc Van Lancker, Metallurgy of Aluminum Alloys, Chapman and Hall, London, UK, 1967.
[14] V.B. John, Engineering Materials, MacMillan Press, UK, 1990.
[15] Z. Huda, Influence of particle mechanisms on the kinetics of grain growth in a P/M superalloy, Mater. Sci. Forum 467–470 (2004) 985.
[16] D. Zhu, W.J. van Ooij, Corros. Sci. 45 (2003) 2163.
[17] R.G. Buchheit, R.P. Grant, P.F. Halva, B. Mekenie, G.I. Zender, J. Electrochem. Soc. 144 (1997) 2621.
[18] G.S. Chen, M. Gao, R.P. Wei, Corrosion 52 (1996) 8.
[19] V. Guillaumin, G. Mankowski, Corros. Sci. 41 (1990) 421.
[20] H.M. Obispo, L.E. Murr, M. Arrowood, E.A. Trillo, J. Mater. Sci. 35 (2000) 3479.
[21] I.N. Khan, M.J. Starink, J.L. Yan, A model for precipitation kinetics and strengthening in Al–Cu–Mg alloys, Mater. Sci. Eng. A 472 (1–2) (2008) 66.